CHEMISTRY OF MATERIALS
Article
Cite This: Chem. Mater. 2017, 29, 9023-9029
pubs.acs.org/cm

Effects of Anion Mobility on Electrochemical Behaviors of Lithium–Sulfur Batteries

Kee Sung Han,*[,†,#] Junzheng Chen,[‡,#] Ruiguo Cao,[‡,#] Nav Nidhi Rajput,[§,#] Vijayakumar Murugesan,[‡,#] Lili Shi,[‡,#] Huilin Pan,[‡,#] Ji-Guang Zhang,*[,‡,#] Jun Liu,[‡,#] Kristin A. Persson,[§,⊥,#] and Karl T. Mueller*[,∥,#]

[†]Environmental Molecular Sciences Laboratory, Pacific Northwest National Laboratory, Richland, Washington 99352, United States
[§]Lawrence Berkeley National Laboratory, Berkeley, California 94720, United States
[‡]Energy and Environmental Directorate, Pacific Northwest National Laboratory, Richland, Washington 99352, Unites States
[∥]Physical and Computational Sciences Directorate, Pacific Northwest National Laboratory, Richland, Washington 99352, United States
[⊥]Department of Materials Science & Engineering, University of California, Berkeley, California 94720-1760, United States
[#]Joint Center for Energy Storage Research (JCESR), Lemont, Illinois 60439, United States

Supporting Information

ABSTRACT: The electrolyte is a crucial component of lithium–sulfur (Li–S) batteries, as it controls polysulfide dissolution, charge shuttling processes, and solid-electrolyte interphase (SEI) layer formation. Experimentally, the overall performance of Li–S batteries varies with choice of solvent system and Li-salt used in the electrolyte, and a lack of predictive understanding about the effects of individual electrolyte components inhibits the rational design of electrolytes for Li–S batteries. Here we analyze the role of the counteranions of common Li salts (such as TfO^-, FSI^-, $TFSI^-$, and TDI^-) when dissolved in DOL/DME (1:1 by vol.) for use in Li–S batteries. The evolution of ion–ion and ion–solvent interactions due to various anions was analyzed using ^{17}O NMR and pulsed-field gradient (PFG) NMR and then correlated with electrochemical performance in Li–S cells. These data reveal that the formation of the passivation layer on the anode and the loss of active materials from the cathode (evidenced by polysulfide dissolution) are related to anion mobility and affinity with lithium polysulfide, respectively. For future electrolyte design, anions with lower mobility and weaker interactions with lithium polysulfides may be superior candidates for increasing the long-term stability of Li–S batteries.

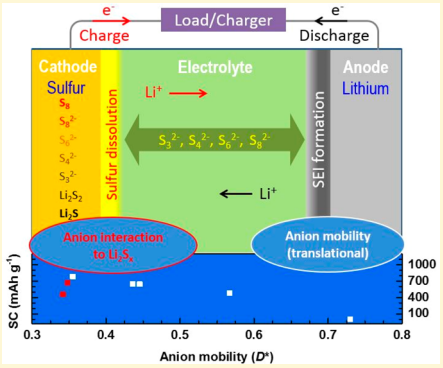

INTRODUCTION

Lithium–sulfur (Li-S) batteries are one of the most promising energy storage device classes as technology moves beyond Li-ion battery systems, due to their higher theoretical energy density (2600 Wh/kg) and specific capacity (1672 mAh/g), coupled with the low cost of sulfur cathode materials.[1,2] However, complex challenges remain, including poor cell performance resulting from the low initial sulfur usage and quick capacity fading due to the generation of highly soluble lithium polysulfides (mostly long chain Li_2S_m, $4 < m \leq 8$) during cycling. To overcome these critical issues, functionalized conductive trappers and additional diffusion barriers (such as carbon hosts and interlayers) have been introduced into these systems.[2] But these additional components reduce the much needed specific capacity and energy density. Hence, recent efforts are mainly focused on designing electrolytes with lower polysulfide solubility.[3] However, a lack of understanding remains about the correlation between Li–S cell performance and electrolyte parameters such as solvent composition, salt concentration, etc. It is necessary, therefore, to correlate the molecular level structure and dynamics of electrolytes to the final battery performance, which can help build basic guidelines for novel or improved electrolyte design. In this work, we analyzed the role of supporting Li salts as it dictates many functional properties of electrolytes. Electrolytes comprised of 1 and 3 M Li salt with various anions—bis(fluorosulfonyl)-imide (FSI^-), triflate (TfO^-), bis(trifluoromethanesulfonyl) imide ($TFSI^-$), and 2-trifluoromethyl-4,5-dicyanoimidazole (TDI^-)—within a DOL/DME (1:1 vol.) solvent mixture were prepared. These electrolyte solutions are denoted as x–y, where x and y represent the salt concentration (i.e., x = 1 or 3) and a type of anion (y = TfO^-, FSI^-, $TFSI^-$, or TDI^-), respectively. In addition, to probe the interaction between dissolved polysulfide species and electrolyte components, we

Received: May 23, 2017
Revised: October 17, 2017
Published: October 17, 2017

DOI: 10.1021/acs.chemmater.7b02105
Chem. Mater. 2017, 29, 9023–9029

added 0.12 M Li_2S_8 into 1 M Li-salt concentration electrolytes and denote these solutions as 1-TfO-PS, 1-FSI-PS, etc. We employed pulsed-field gradient (PFG) NMR and natural abudance ^{17}O NMR spectrocscopy to interrogate ion−ion/ion−solvent interactions and the subsequent ion/solvent diffusion process. The Li−S cells fabricated with these electrolytes were tested, and their specific capacities (SCs) are correlated with molecular level ion solvate structure.

EXPERIMENTAL METHODS

Sample Preparations. The 1 and 3 M solutions were prepared by dissolution of the appropriate Li salts containing the anions, trifluoromethanesulfonate (TfO^-), bis(fluorosulfonyl)imide (FSI^-), bis(trifluoromethane)sulfonimide ($TFSI^-$), and 2-trifluoro-4,5-dicyanoimidazolide (TDI^-), in mixture of 1,3-dioxolane (DOL) and dimethoxyethane (DME) (DOL/DME, 1:1 vol.). In addition, 0.12 M polysulfide (Li_2S_8) was added into 1 M solutions. Nominal Li_2S_x solutions were obtained by mixing stoichiometric Li_2S and S_8 within the electrolyte and stirring at 60 °C in an oil bath overnight inside of a glovebox. The ionic conductivities of 1 M electrolyte solutions were measured using a conductivity meter (Orion 3 Star, Thermo Scientific) at 30 °C.

Electrochemical Characterization. Li−S battery cells using the electrolytes described above were fabricated using 64% sulfur (purity ≥ 99.5% from Sigma-Aldrich), 16% multiwalled carbon nanotubes (MWCNT) (Cheap Tubes Inc.), 10% super P carbon additive, and 10% polyvinylidene fluoride (PVDF) binder. The sulfur/MWCNT composite was prepared by a melt-diffusion approach. Sulfur powder and MWCNTs in a weight ratio of 4:1 were mixed in a mortar by hand, and then the mixture was transferred to a Teflon-lined stainless steel autoclave and heat treated at 155 °C in a furnace for 24 h to improve the sulfur distribution inside the MWCNTs matrix, resulting in a S80/MWCNTs20 composite. The sulfur cathode was prepared by coating the *N*-methyl-2-pyrrolidone (NMP) slurry of S80/MWCNTs20 composite, conductive carbon, and PVDF binder with a weight ratio of 8:1:1 onto an aluminum foil. After the NMP was evaporated inside a fume hood, the sulfur cathode was punched into discs (7/16 in.) and further dried in a vacuum oven at 60 °C. The sulfur mass loading of the electrode was approximately 1 mg/cm^2. The half cell (coin cell 2320) was assembled in an Ar-filled glovebox with a Li metal anode and cycled at a range of 1.5−3 V at 0.2 C (1 C = 1675 mA/g of S). The specific capacity (SC) was calculated based on sulfur weight. Further details of electrochemical cell preparation and testing were reported earlier.[4,5]

Nuclear Magnetic Resonance (NMR) Spectroscopy and Pulsed Field Gradient (PFG) NMR. ^{17}O NMR spectra were obtained using single pulse excitation at ambient temperature. Diffusion coefficients of Li^+, anions, and solvent molecules (DOL and DME) were measured using ^7Li, ^{19}F, and ^1H PFG-NMR with a convection compensation PFG sequence (Dbppste_cc in VNMRJ 3.2, Agilent) in the temperature range from 0 to 50 °C. All NMR experiments were performed on a 600 MHz NMR spectrometer (Agilent) equipped with a 5 mm liquid/diffusion NMR probe (Doty Scientific Instrument, U.S.A.), which has the maximum gradient strength of ∼31 T/m. The ionic conductivity, σ_D, was calculated by the Nernst−Einstein equation[6]

$$\sigma_D\ (\mathrm{S\ cm^{-1}}) = \frac{e^2}{k_B T}(n_{Li}D_{Li} + n_{anion}D_{anion}) \quad (1)$$

where e is the elementary charge and n is the number of ions in the unit volume of V_m, meaning that $n = (N_A \cdot x)/V_m$, where N_A, x, and V_m are Avogadrò number, ion concentration, and molar volume, respectively.

RESULTS AND DISCUSSION

The diffusion coefficients of Li^+ cations (D_{Li}), anions (D_{anion}), and solvent molecules DME (D_{DME}) and DOL (D_{DOL}) were measured in the temperature range of 0 to 50 °C (Figure S1). All electroytes appear to obey the Stokes−Einstein theory of diffusion, i.e., $D = k_B T/f$, where diffusion coefficient (D) is inversely proportional to the friction factor $f = 6\pi\eta r_s$ and η and r_s are the viscosity and hydrodynamic radius of diffusing molecules (i.e., radius of the hard solvation sphere that diffuses along with solute), respectively.[7] Figure 1 shows diffusion

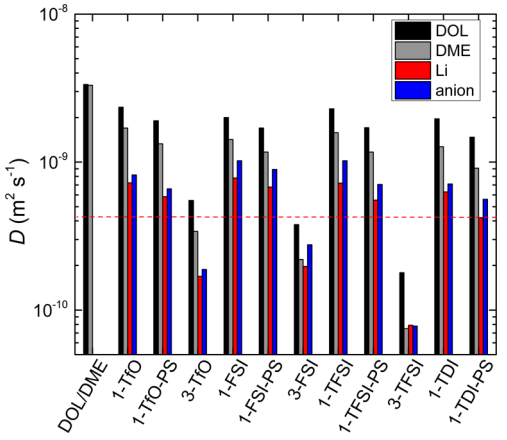

Figure 1. Diffusion coefficients of Li^+ (D_{Li}), anion (D_{anion}), DOL (D_{DOL}), and DME (D_{DME}) for the electrolytes consisting of 1 or 3 M Li salt (LiTfO, LiFSI, LiTFSI, or LiTDI) dissolved in DOL/DME (1:1 vol.) and 1 M Li salt dissolved in DOL/DME with 0.12 M Li_2S_8, all obtained at 50 °C.

coefficients of various electrolytes measured at 50 °C. It is interesting to note that $D_{DME} \approx D_{DOL}$ in the neat DOL/DME solvent system, despite their obvious molecular size differences. This similarity implies that the intermolecular interaction in this solvent mixture is very small, and hence the hydrodynamic radii (r_s values) of DOL and DME simply represent their polar surface areas (A_p), i.e., the surface belonging to polar atoms, which is reported to be similar ($A_p \sim 18.5$ Å^2) (Figure S2).[8] The theoretical r_{DOL} and r_{DME} values were estimated to be 2.43 Å ($r = (A_P/\pi)^{1/2}$). Each value for r_x was calculated from the volume of the anion and is reported in Table 1. The diffusion

Table 1. Radius, $r = (3V/4\pi)^{1/3}$, Where V Is Volume of Anions,[11] Ionic Conductivity, σ_{meas}, and Calculated Ionic Conductivity, σ_D, Using Diffusion Coefficients at 30 °C

anions	r (Å)	σ_D (S cm^{-1})	σ_{meas} (S cm^{-1})	σ_{meas}/σ_D
FSI^-	3.27	5.1×10^{-2}	1.7×10^{-2}	0.34
TfO^-	2.95	4.4×10^{-2}	2.6×10^{-3}	0.06
$TFSI^-$	3.53	4.2×10^{-2}	1.1×10^{-2}	0.26
TDI^-	3.46[10]	2.4×10^{-2}	6.2×10^{-3}	0.26

coefficients of all electrolyte components including solvent molecules were considerably reduced with introduction of Li salts (both at 1 and 3 M concentrations) and 0.12 M Li_2S_8. However, D_{DME} drops more significantly than D_{DOL} for all electrolyte solutions, suggesting that DME molecules are more actively participating in the Li^+-solvation process than the DOL molecules as predicted by our compuational modeling (Figure S3).

This preferential Li^+-solvation by DME molecules can be confirmed by ^{17}O NMR spectroscopy based on its known sensitivity to molecular interactions with Li^+ cations.[9] Unlike the DOL molecules, DME molecules showed a noticeable

DOI: 10.1021/acs.chemmater.7b02105
Chem. Mater. 2017, 29, 9023−9029

upfield chemical shift $\delta(^{17}O)$ with the introduction of Li salt and Li_2S_8, corroborating the preferential DME solvation around Li^+ cations (Figure S4). By correlating the upfield shift in DME resonance with choice of anions, the interaction strength of DME molecules with Li^+ cations increases as a function of anion in the following order: TfO^- < FSI^- < $TFSI^-$ < TDI^- (see Figure S4a). At 1 M Li-salt concentration, the DME registers a single resonance indicating relatively faster solvent exchange between solvate structure and bulk solvent. However, at 3 M Li-salt concentrations an additional ^{17}O peak from DME arises significantly downfield (Figures S4 and S5), indicating the agglomeration of Li^+-DME solvation shells (i.e., an aggregated solvate structure) due to fewer bulk solvent molecules at higher salt concentrations.[12] The population of these aggregated Li^+-solvate structures tends to increase with salt concentrations as evidenced by an even further downfield ^{17}O shift of DME for 4-TfO and 4-FSI electrolytes (Figure S4). This larger downfield ^{17}O shift of DME may be due to (1) reduced (local) dielectric constant (ε) within the aggregated Li^+-solvate clusters[13−16] relative to the bulk ε values representing free DME and DOL molecules or (2) restricted DME solvent exchange dynamics due to the bidentate complexation within Li^+-solvate clusters.[16] To further evaluate these hypotheses we performed classical molecular dynamics (MD) simulations for the 3-TFSI system (see Supporting Information), and Figure 2 shows a snapshot of solvate

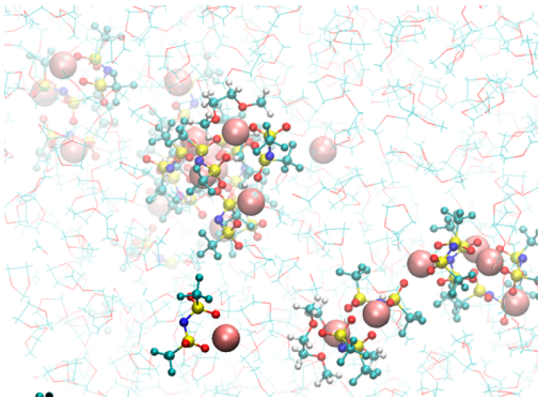

Figure 2. Snapshot of solvate structural evolution calculated in 3 M LiTFSI dissolved in DOL/DME obtained from molecular dynamics simulation.

structural evolution. This analysis reveals that at higher salt concentrations the Li-clustering is predominantly due to the scarcity of bulk solvent molecules and overlapping Li^+ solvation spheres. In addition, bidentate complex formation (based on Li−DME interactions) is also evident. This observation supports the variation in ^{17}O NMR chemical shift and line broadening observed at higher salt concentrations. In addition, a weaker Li^+−DOL interaction was also observed. The integrated intensity of this downfield ^{17}O peak from DME depends linearly on the molecular size of the anions (Figure S5), which suggests that the identity of the anion clearly influences the formation of aggregates and subsequent solvate structural evolution. In addition, the $\delta(^{17}O)$ of the remaining DME molecules in 3-TfO and 3-FSI electrolytes register further upfield shifts relative to lower concentration (1 M) samples. This observation reflects the salt concentration. For example, the intensity of the ^{17}O peak from the $TFSI^-$ anion in 3-TFSI is about 20% of that from DOL molecules, while it should be ∼1.3 times larger based on the ratio of oxygen atoms between $TFSI^-$ and DOL. Such a significant drop in ^{17}O peak intensity might be a result of heavy peak broadening due to stronger interaction between Li^+ and DME as a function of increasing Li salt concentration. In addition, the integrated intensities of ^{17}O resonances from TfO^- and $TFSI^-$ anions are much smaller than those expected from the electrolyte with 3 M concentration due to immobility of anions in the system. This observation implies that the TfO^- and $TFSI^-$ anions actively participate in agglomerated solvate clusters with Li^+, leading to diminished mobility within concentrated electrolytes. On the other hand, the FSI^- molecules retains its ^{17}O peak intensity, indicating relatively weaker interactions and higher mobility within their solvate structures. This molecular level view of electrolyte solution structure derived from an ^{17}O chemical shift analysis helps us derive an evolving mesoscale view of the diffusion process and its effect on Li−S cell performance.

On the basis of the diffusion measurements and ^{17}O chemical shift analysis, it is clear that the interactions of DOL molecules with other components of the electrolyte are relatively weaker. Hence, the hydrodynamic radius of DOL molecules ($r_{s,DOL}$) will be similar to its actual molecular size (i.e., $r_{s,DOL} \approx r_{DOL}$) within all electrolytes discussed here. Therefore, the variation of D_{DOL} in these electrolytes is primarily due to a change in viscosity resulting from the unique interactions between the electrolyte components, similar to the D of hydrofluoroether in the LiTFSI dissolved in a mixture of triglyme and hydrofluoroether (Figure S6).[17] It is difficult to confirm the weaker intermolecular interaction of DOL through viscosity (η^{-1}) analysis due to the large uncertainty of the measured viscosity values (Figure S6a). Evidently, the literature reported viscosity values are sporadic for similar electrolyte systems. For example, the viscosity of 3 M LiTFSI dissolved in DOL/DME was reported to be 25.9,[5] 16.12,[18] and 8.8[19] mPa·s at 25 °C. For 1 M LiTFSI dissolved in DOL/DME, viscosities are similarly widely variant in the literature, reported as 2.56,[18] 2.03,[19] and 1.35[4] mPa·s at 25 °C. Nevertheless, these electrolytes obey the Stokes−Einstein relation of diffusion from the proportionality of D and η^{-1} (Figure S6a). Therefore, we performed classical molecular dynamics (MD) calculations, which confirm the weak intermolecular interaction of DOL (Figure 2). In particular, the interaction of DOL with Li^+ cations is much smaller than that of Li^+−TFSI and Li^+−DME based on radial distribution function (RDF) analysis (Figure S7), thereby confirming our hypothesis that DOL establishes and experiences weaker intermolecular interactions. Hence the measured value of D_{DOL} can be used to derive the viscosity-normalized mobility of Li^+ cations (D_{Li}/D_{DOL}), anions (D_{anion}/D_{DOL}), and DME molecules (D_{DME}/D_{DOL}) because D of each of the components obey the Stokes−Einstein relation. These inherent mobilities of ions and solvent molecules are then correlated with the specific capacity (see Figure 3) obtained at the 33rd and 100th cycle for Li−S batteries fabricated with the respective electrolytes (Figure S8). The long-term SC and the capacity decay rate, ΔSC (%)—obtained from the SC difference between 33rd and 100th cycle—depend strongly on the anion mobility (D_{anion}/D_{DOL}) except for electrolytes containing the TfO^- anion. Surprisingly, the mobilities of Li^+ cations (Figure 3c,d) or the solvent (DME) molecules (Figure S9) do not follow a linear correlation with SC or ΔSC. Apparently, the slower anion mobility within the electrolyte can help in achieving stable cycling of a Li−S cell. However, it should be

DOI: 10.1021/acs.chemmater.7b02105
Chem. Mater. 2017, 29, 9023−9029

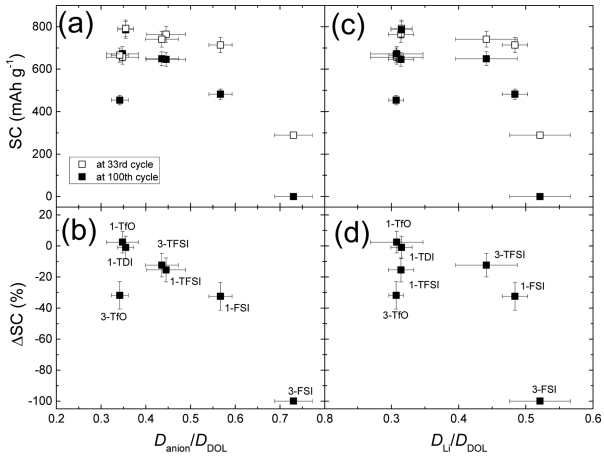

Figure 3. (a) Specific capacity, SC, at the 33rd and 100th cycles and (b) SC decay (ΔSC) from the 33rd to 100th cycle in Li–S batteries fabricated with the electrolytes composed of 1 or 3 M Li salt (LiFSI, LiTfO, LiTFSI, or LiTDI) dissolved in DOL/DME (1:1 vol.) plotted as a function of D_{anion}/D_{DOL}. The same functions are plotted as a function of D_{Li}/D_{DOL} in (c) and (d).

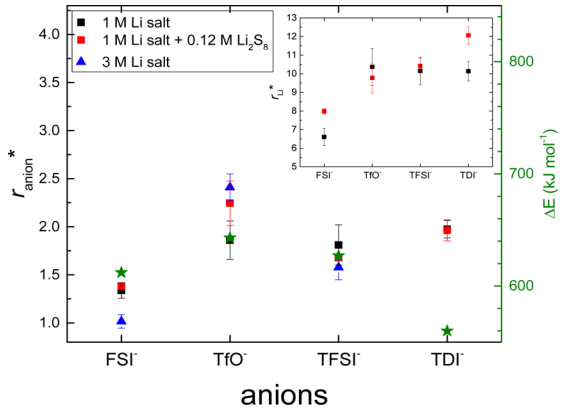

Figure 4. Effective hydrodynamic radius of anions, r_{anion}*, for these electrolytes and Li^+ cation–anion binding energy, ΔE (green stars), from DFT calculations.[11,20] The inset shows the r_{Li}* values for these electrolytes.

noted that electrolytes with TfO^- anion show poor performance despite their slower mobility. Obviously, anion mobility might be one of the factors in determining the long-term SC of Li–S cell performance.

To gain a deeper understanding of the role of electrolyte components on Li–S cell performance, we compared various ion–ion/ion–solvent interactions estimated from the variation of the ratio of hydrodynamic radius to actual molecular radii, $r_{s,x}/r_x \equiv r_x$*, the so-called "effective hydrodynamic radius", where x is the Li^+ cation, the anion, or DME. This quantity can be calculated using the fact that $r_{s,DOL} \approx r_{DOL}$ as discussed earlier. The ratio D_x/D_{DOL} obtained from the same solution will be proportional to the ratio of the hydrodynamic radii ($r_{s,DOL}/r_{s,x}$) between x and DOL based on the Stokes–Einstein equation. If both x and DOL are isolated from other components of the electrolyte, then the ratio D_x/D_{DOL} will be proportional to r_{DOL}/r_x, where r_{DOL} and r_x are the actual molecular size of DOL and x, respectively. But only DOL molecules appear to be isolated from other electrolyte components. Then the interaction strength of component x to other components of the electrolyte, r_x*, will be $(r_{DOL}/r_x)/(r_{s,DOL}/r_{s,x}) = r_{s,x}/r_x$. *Therefore, determining values of* r_x* *of various electrolyte components will provide insight into the various intermolecular interactions such as ion–ion and ion–solvent interaction strengths within electrolyte systems.* For example, if a solvent/ion has weaker interaction with other components of the electrolyte, then the r_x* will be close to unity as observed for FSI^- anion (i.e., r_{FSI}* ≈ 1) in the 3-FSI electrolyte (see Figure 4). Conversely, Li^+ cations register significantly higher values of r_{Li}* (inset of Figure 4), due to their preferred interaction with both solvent and anion molecules as part of the solvation phenomena. This is also evidenced by higher r_{DME}* values observed for the solvent DME molecules (Figure S10). Similarly, r_{anion}* is higher for all other anions (r_{anion}* > 1) at various electrolyte compositions, indicating that ion–ion type interactions between Li^+ and anions (i.e., contact-ion pair formation) is crucial in solvate structure formation. Solvate structures with significant contact-ion pair formation (which will depend on the Li^+ affinity of a particular anion) can critically influence their mobilities within electrolytes and subsequently affect the final Li–S cell performance. Apparently, the trend of Li^+-anion association energy calculated by density functional theory[11,20] for various anions follows the r_{anion}* value for 1 M Li salts except for the TDI^- anion. However, previous experimental analysis has shown that the coordination tendency of TDI^- anion to Li^+ cation in DME solvent is stronger than that of $TFSI^-$ anion and is similar to that of TfO^- anion,[21] which is in good agreement with our observations of r_{anion}*. This fact reinforces the hypothesis that contact-ion pair formation can be predicted by consideration of r_{anion}* for electrolyte solutions. For example, the effective hydrodynamic radius of TfO^- (r_{TfO}*) increases with salt concentration (i.e., comparing 1- and 3-TfO electrolytes) while other anions display similar or lower values with increase in Li salt concentration. In addition, the r_{TfO}* value increases with the introduction of Li_2S_8 suggesting that TfO^- anions strongly interact with both Li^+ as well as Li_2S_8 through contact-ion pair formation. This TfO^- anion based contact-ion pair formation is also reflected in the largest r_{Li}* (inset of Figure 4) and the smallest r_{DME}* value among the various electrolyte systems (Figure S10). Interestingly, with the introduction of Li_2S_8 the values of r_{Li}* are significantly reduced, suggesting preferential interaction of TfO^- anions with lithium polysulfide species[22,23] and subsequent polysulfide dianion (S_n^{2-}) formation through $Li_2S_x + TfO^- = Li^+–TfO^- + S_x^{2-}$ as reported earlier.[24] Conversely, r_{Li}* values for other anions were increased with addition of Li_2S_8 indicating their weaker interaction with the Li^+ cations of Li_2S_8. In particular electrolytes containing TDI^- anions register relatively larger increments of r_{Li}* by addition of Li_2S_8, suggesting that the TDI^- anion interaction to lithium polysulfide is weakest among these electrolytes and the solubility of lithium polysulfides is restricted.[4]

The role of DME solvent molecules in solvation structure can be analyzed by the variation of r_{DME}* with various anions and salt concentrations. It is interesting to note that r_{DME}* is influenced by the Li-salt concentration but not affected by the addition of Li_2S_8 (Figure S10). Therefore, the DME solvent molecules are not directly participating in the dissociation of lithium polysulfide species in the electrolyte (unlike the behavior and effect of the anions) but rather mainly solvate the Li-salt. In fact, this conjecture explains the relatively lower solubility of lithium polysulfide in a neat DME solvent system. However, the Li^+-DME interaction strength can still be influenced by the anions as detected by the evolution of

DOI: 10.1021/acs.chemmater.7b02105
Chem. Mater. 2017, 29, 9023–9029

r_{DME}* and the DME $\delta(^{17}O)$ chemical shifts (see Figures S4, S5, and S10). To test the influence of anions (in terms of contact-ion pair formation) on the Li^+-DME interaction strength, we measured ionic conductivity (σ_{meas}) and compared these measured values with those derived from diffusion coefficients (σ_D) using the Nernst–Einstein equation[6] (see Table 1). As expected the σ_{meas}/σ_D is smaller than unity for all electrolytes due to the assumption of complete ion dissociation (i.e., variant solute–solvent interactions including contact-ion pair formation are not included) in the calculation of σ_D. Hence, the σ_{meas}/σ_D ratio mainly reflects the degree of Li^+–anion dissociation. Interestingly, the 1-TfO solution shows the smallest σ_{meas}/σ_D value indicating relatively stronger interaction of TfO^- anion with Li^+ cations as predicted by the variation of r_{TfO}* as well as by r_{Li}* (see Figure 3). In contrast, the FSI^- anion shows a higher degree of Li^+–anion dissociation among the electrolytes with 1 M Li salt concentration. However, the σ_{meas}/σ_D ratio for these electrolytes is not in good agreement with that of the Li^+–DME interaction strength estimated from $\Delta\delta(^{17}O)$ and variations of r_{DME}* discussed earlier. This observation means that the degree of Li^+–anion contact-ion pair formation is not related to the Li^+–DME interaction strength (at least for lower concentration electrolytes). As discussed earlier, the effective hydrodynamic radius of the anion (r_{anion}*) rather than the DME ^{17}O chemical shift analysis can provide details of anion specific contact-ion pair formation.

The battery SC (at the 100th cycle) plotted as a function of r_{anion}* (Figure 5) clearly shows that the long-term SC of Li–S batteries increases with the strength of anion interactions as well as its anion mobility (Figure 3) because D_{anion} is inversely proportional to hydrodynamic radius ($D_{anion} \propto 1/r_{s,anion}$). However, the 3-TfO electrolyte registers significantly lower SC than expected due to the strong interaction of the anions with Li^+. This low SC might be due to significant loss of active materials from the cathode as a consequence of the strong interaction of TfO^- anions with lithium polysulfides as predicted by higher r_{anion}* and lower r_{Li}* values in TfO^- containing electrolyte with Li_2S_8 (Figure 4).[22,23] This is clearly seen when the SC of a Li–S cell composed of 1-TfO electrolyte is plotted vs r_{anion}* calculated from electrolytes with 1 M Li salt concentration that also contained 0.12 M Li_2S_8. The lower SC for the 1-TfO electrolyte is due to its higher r_{anion}*. In addition, the decay of SC will be more accelerated in the higher LiTfO concentration electrolyte (Figure 3b), due to the preference of TfO^- anion for interactions with polysulfide, leading to enhanced loss of active materials from the cathode. Conversely, electrolytes containing the FSI^- anion with both 1 and 3 M concentrations show poor cell performance (Figures 3 and 5). In fact, the Li–S battery fabricated with 3-FSI electrolyte failed abruptly at the 34th cycle, which we suggest is due to the fast formation of an insulating passivation layer on the Li-metal anode as observed previously.[5,22,25] Images from SEM analyses confirmed thick SEI layer formation on the Li anode surfaces from the Li–S battery fabricated with 3-FSI. The thickness of the SEI layer after the 33rd cycle in the 3-FSI battery was similar to that from the anode of the 3-TFSI battery after its 200th cycle.[5] In addition, the Li–S cell fabricated with 3-FSI shows significantly increased impedance as a function of extended charging/discharge cycles.[5] This observation strongly suggests that the anion, which has higher mobility and relatively weaker interaction with other electrolyte components, can easily participate in the chemical reaction at Li-metal anode surfaces as part of SEI layer formation. The overall result showed that both SC and ΔSC of Li–S batteries depend strongly on the anion mobility (Figure 3) which is directly linked to its interactions with other electrolyte components. However, electrolytes containing both TfO^- and FSI^- anions register lower long-term SC and larger ΔSC than expected from their mobilities and Li^+-anion interaction strengths. Therefore, the poor Li–S cycling performance of these two electrolytes might originate from two different and competing aspects of anion mobility. For the FSI^- anions, their higher mobility may enhance their interaction with Li metal anode surfaces and cause accelerated detrimental SEI layer formation. On the other hand, and despite its lower mobility, the TfO^- anion can exert stronger interactions with lithium polysulfide thereby accelerating detrimental polysulfide dissolution from the cathode, especially at higher LiTfO concentrations. Interestingly, the TDI^- anion exhibits better Li–S cell performance due to its relatively lower mobility and weaker interaction with lithium polysulfides. Overall, the anion plays a critical role in SEI layer formation as well as the polysulfide dissolution process, which are critical factors affecting Li–S cell performance. A highly mobile anion (due to its weaker interaction with Li^+ cations) can lead to higher concentration of anions at Li–electrolyte interfaces resulting in enhanced salt decomposition and subsequent formation of a thick passivating SEI layer. Conversely, a lower mobility anion (due to its relatively stronger interaction with Li^+ cations) can result in preferential interaction with lithium polysulfides and enhance the detrimental polysulfide dissolution process.

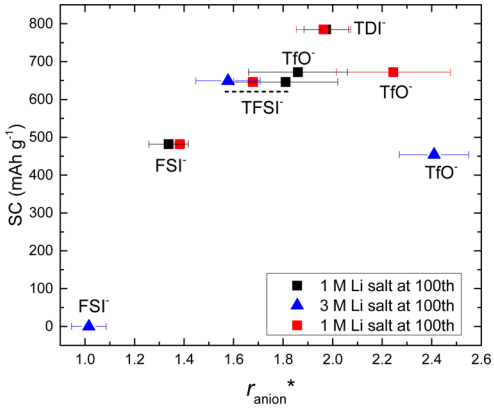

Figure 5. Specific capacity (SC) of Li–S batteries fabricated with the electrolytes composed of 1 or 3 M Li salt (LiFSI, LiTfO, LiTFSI, or LiTDI) dissolved in DOL/DME (1:1 by vol.) at the 100th cycle plotted as a function of r_{anion}*. The red squares report measurements of SC as a function of r_{anion}* obtained from 1 M Li salt dissolved in DOL/DME with 0.12 M Li_2S_8.

CONCLUSIONS

We measured diffusion coefficients of each of the components of Li–S electrolytes composed of different anions (FSI^-, TfO^-, $TFSI^-$, and TDI^-) and correlated these results with Li–S cell performance. The various ion–ion and ion–solvent interactions can influence the anion mobility within electrolytes and thereby influence the final Li–S cell performance. The correlation between diffusion measurements and the specific capacity reveals that the anion mobility as well as interaction strength with Li^+ cations are crucial in designing electrolytes for Li–S cells. The higher mobility of an anion (such as FSI^-) due to weaker interactions with other electrolyte components often

DOI: 10.1021/acs.chemmater.7b02105
Chem. Mater. 2017, 29, 9023–9029

leads to the formation of a thicker passivation layer, whereas strongly interacting anions (such as TfO^-) can accelerate polysulfide dissolution due to their preferential interaction with lithium polysulfides. These predictions are validated by the relatively better cell performance of TDI^- based electrolyte, where the TDI has lower mobility and weak interactions with lithium polysulfide. Based on this observation, the optimal electrolyte should contain anions with lower mobilities as well as weaker interaction strengths toward polysulfide. Nevertheless, we realize that the complex nature of the solvation phenomenon within electrolyte under realistic cell operating conditions needs to be further analyzed to build advanced strategies for electrolyte design.

■ ASSOCIATED CONTENT

Supporting Information

The Supporting Information is available free of charge on the ACS Publications website at DOI: 10.1021/acs.chemmater.7b02105.

MD simulations, materials, temperature dependent diffusion coefficients, molecular structures of anions and solvents, ^{17}O NMR spectra, specific capacity retention plots, etc. (PDF)

■ AUTHOR INFORMATION

Corresponding Authors

*(K.S.H.) E-mail: keesung.han@pnnl.gov.
*(K.T.M.) E-mail: karl.mueller@pnnl.gov.
*(J.-G.Z.) E-mail: jiguang.zhang@pnnl.gov.

ORCID

Kee Sung Han: 0000-0002-3535-1818
Nav Nidhi Rajput: 0000-0003-4740-8217
Vijayakumar Murugesan: 0000-0001-6149-1702
Ji-Guang Zhang: 0000-0001-7343-4609
Jun Liu: 0000-0001-8663-7771
Karl T. Mueller: 0000-0001-9609-9516

Notes

The authors declare no competing financial interest.

■ ACKNOWLEDGMENTS

We acknowledge Prof. Dr. J. Scheers at Chalmers University of Technology (Sweden) for the calculation of TDI^- anion size. The Materials Engineering Research Facility (MERF) at Argonne National Laboratory is greatly appreciated for the redistribution of LiTDI. The authors thank Dr. Masashi Yukitake and Dr. Kazuhiko Murata (Nippon Shokubai Co., Ltd.) for providing LiFSI salt for viscosity measurements. This research was led intellectually by researchers within the Joint Center for Energy Storage Research (JCESR), an Energy Innovation Hub funded by the U.S. Department of Energy (DOE), Office of Science, Basic Energy Sciences (BES). The classical molecular dynamics simulations were performed using the computational resources of the National Energy Research Scientific Computing Center (NERSC), which is supported by the Office of Science of the U.S. Department of Energy under Contract No. DE-AC02-05CH11231. The NMR measurements were performed at the Environmental Molecular Sciences Laboratory (EMSL), a national scientific user facility sponsored by the DOE's Office of Biological and Environmental Research and located at Pacific Northwest National Laboratory (PNNL).

■ REFERENCES

(1) Yin, Y.-X.; Xin, S.; Guo, Y.-G.; Wan, L.-J. Lithium−Sulfur Batteries: Electrochemistry, Materials, and Prospects. *Angew. Chem., Int. Ed.* **2013**, *52*, 13186−13200.
(2) Manthiram, A.; Fu, Y.; Chung, S.-H.; Zu, C.; Su, Y.-S. Rechargeable Lithium−Sulfur Batteries. *Chem. Rev.* **2014**, *114*, 11751−11787.
(3) Zhang, S.; Ueno, K.; Dokko, K.; Watanabe, M. Recent Advances in Electrolytes for Lithium-Sulfur Batteries. *Adv. Energy Mater.* **2015**, *5*, 1500117.
(4) Chen, J.; Han, K. S.; Henderson, W. A.; Lau, K. C.; Vijayakumar, M.; Dzwiniel, T.; Pan, H.; Curtiss, L. A.; Xiao, J.; Mueller, K. T.; Shao, Y.; Liu, J. Restricting the Solubility of Polysulfides in Li-S Batteries Via Electrolyte Salt Selection. *Adv. Energy Mater.* **2016**, *6*, 1600160.
(5) Cao, R.; Chen, J.; Han, K. S.; Xu, W.; Mei, D.; Bhattacharya, P.; Engelhard, M. H.; Mueller, K. T.; Liu, J.; Zhang, J.-G. Effect of the Anion Activity on the Stability of Li Metal Anodes in Lithium-Sulfur Batteries. *Adv. Funct. Mater.* **2016**, *26*, 3059−3066.
(6) Hayamizu, K. Temperature Dependence of Self-Diffusion Coefficients of Ions and Solvents in Ethylene Carbonate, Propylene Carbonate, and Diethyl Carbonate Single Solutions and Ethylene Carbonate + Diethyl Carbonate Binary Solutions of LiPF6 Studied by NMR. *J. Chem. Eng. Data* **2012**, *57*, 2012−2017.
(7) Pregosin, P. S.; Kumar, P. G. A.; Fernández, I. Pulsed Gradient Spin−Echo (PGSE) Diffusion and ^1H, ^{19}F Heteronuclear Overhauser Spectroscopy (HOESY) NMR Methods in Inorganic and Organometallic Chemistry: Something Old and Something New. *Chem. Rev.* **2005**, *105*, 2977−2998.
(8) National Center for Biotechnology Information. http://pubchem.ncbi.nlm.nih.gov (accessed August 2015).
(9) Bogle, X.; Vazquez, R.; Greenbaum, S.; Cresce, A. v. W.; Xu, K. Understanding Li^+−Solvent Interaction in Nonaqueous Carbonate Electrolytes with ^{17}O NMR. *J. Phys. Chem. Lett.* **2013**, *4*, 1664−1668.
(10) Scheers, J. Private communication, July 2015.
(11) Johansson, P. Electronic structure calculations on lithium battery electrolyte salts. *Phys. Chem. Chem. Phys.* **2007**, *9*, 1493−1498.
(12) Seo, D. M.; Borodin, O.; Han, S.-D.; Boyle, P. D.; Henderson, W. A. Electrolyte Solvation and Ionic Association II. Acetonitrile-Lithium Salt Mixtures: Highly Dissociated Salts. *J. Electrochem. Soc.* **2012**, *159*, A1489−A1500.
(13) Gerothanassis, I. P. Oxygen-17 NMR spectroscopy: Basic principles and applications (Part I). *Prog. Nucl. Magn. Reson. Spectrosc.* **2010**, *56*, 95−197.
(14) Renou, R.; Ding, M.; Zhu, H.; Szymczyk, A.; Malfreyt, P.; Ghoufi, A. Concentration Dependence of the Dielectric Permittivity, Structure, and Dynamics of Aqueous NaCl Solutions: Comparison between the Drude Oscillator and Electronic Continuum Models. *J. Phys. Chem. B* **2014**, *118*, 3931−3940.
(15) Levy, A.; Andelman, D.; Orland, H. Dielectric Constant of Ionic Solutions: A Field-Theory Approach. *Phys. Rev. Lett.* **2012**, *108*, 227801.
(16) Jankowski, P.; Dranka, M.; Wieczorek, W.; Johansson, P. TFSI and TDI Anions: Probes for Solvate Ionic Liquid and Disproportionation-Based Lithium Battery Electrolytes. *J. Phys. Chem. Lett.* **2017**, *8*, 3678−3682.
(17) Moon, H.; Mandai, T.; Tatara, R.; Ueno, K.; Yamazaki, A.; Yoshida, K.; Seki, S.; Dokko, K.; Watanabe, M. Solvent Activity in Electrolyte Solutions Controls Electrochemical Reactions in Li-Ion and Li-Sulfur Batteries. *J. Phys. Chem. C* **2015**, *119*, 3957−3970.
(18) Hu, J. J.; Long, G. K.; Liu, S.; Li, G. R.; Gao, X. P. A LiFSI-LiTFSI binary-salt electrolyte to achieve high capacity and cycle stability for a Li-S battery. *Chem. Commun.* **2014**, *50*, 14647−14650.
(19) Zhang, Y. Z.; Liu, S.; Li, G. C.; Li, G. R.; Gao, X. P. Sulfur/polyacrylonitrile/carbon multi-composites as cathode materials for lithium/sulfur battery in the concentrated electrolyte. *J. Mater. Chem. A* **2014**, *2*, 4652−4659.
(20) Scheers, J.; Johansson, P.; Szczeciński, P.; Wieczorek, W.; Armand, M.; Jacobsson, P. Benzimidazole and imidazole lithium salts for battery electrolytes. *J. Power Sources* **2010**, *195*, 6081−6087.

DOI: 10.1021/acs.chemmater.7b02105
Chem. Mater. 2017, 29, 9023−9029

(21) McOwen, D. W.; Delp, S. A.; Paillard, E.; Herriot, C.; Han, S.-D.; Boyle, P. D.; Sommer, R. D.; Henderson, W. A. Anion Coordination Interactions in Solvates with the Lithium Salts LiDCTA and LiTDI. *J. Phys. Chem. C* **2014**, *118*, 7781−7787.
(22) Park, J.-W.; Ueno, K.; Tachikawa, N.; Dokko, K.; Watanabe, M. Ionic Liquid Electrolytes for Lithium−Sulfur Batteries. *J. Phys. Chem. C* **2013**, *117*, 20531−20541.
(23) Ueno, K.; Park, J.-W.; Yamazaki, A.; Mandai, T.; Tachikawa, N.; Dokko, K.; Watanabe, M. Anionic Effects on Solvate Ionic Liquid Electrolytes in Rechargeable Lithium−Sulfur Batteries. *J. Phys. Chem. C* **2013**, *117*, 20509−20516.
(24) Vijayakumar, M.; Govind, N.; Walter, E.; Burton, S. D.; Shukla, A.; Devaraj, A.; Xiao, J.; Liu, J.; Wang, C.; Karim, A.; Thevuthasan, S. Molecular structure and stability of dissolved lithium polysulfide species. *Phys. Chem. Chem. Phys.* **2014**, *16*, 10923−10932.
(25) Kim, H.; Wu, F. X.; Lee, J. T.; Nitta, N.; Lin, H. T.; Oschatz, M.; Cho, W. I.; Kaskel, S.; Borodin, O.; Yushin, G. In Situ Formation of Protective Coatings on Sulfur Cathodes in Lithium Batteries with LiFSI-Based Organic Electrolytes. *Adv. Energy Mater.* **2015**, *5*, 1401792.

DOI: 10.1021/acs.chemmater.7b02105
Chem. Mater. 2017, 29, 9023−9029